

# CO combustion catalyst for micro gas sensor application

M. Nishibori · W. Shin · N. Izu · T. Itoh ·  
I. Matsubara

Received: 16 March 2010/Accepted: 31 August 2010/Published online: 15 September 2010  
© Springer Science+Business Media, LLC 2010

**Abstract** CO combustion catalysts of Au loaded on  $\text{Co}_3\text{O}_4$  which contains high concentration of Au (3, 10, 20, and 40 wt%) for the integration on the microdevice were developed and the combustion performance of these catalysts were evaluated. The highly dispersed Au/ $\text{Co}_3\text{O}_4$  catalyst was prepared using the mechanical mixing of the Au colloid (average particle size of 3 nm) and a cobalt oxide powder (particle size of 20–30 nm). The catalyst preparation by the colloid process could result a better dispersion of Au particles in the Au/ $\text{Co}_3\text{O}_4$  catalyst. The Au particle size of the Au content of 20 wt% was 1/10 of that by the catalyst of same composition prepared by impregnation process in our previous studies. This improvement of microstructure enhanced the combustion performance of the catalyst, which was improved 10 times as compared to that of our previous study. Moreover, the CO selectivity of the Au/ $\text{Co}_3\text{O}_4$  catalyst on the microdevice depended on the Au particle size.

## Introduction

Micro-thermoelectric gas sensor (micro-TGS) is operating on the basis of the oxidation of flammable gas by a catalyst combustor, similar to the catalytic-combustion-type gas sensor, so that the sensor performance depends on the activity of the catalyst. We have reported that the micro-TGS

with Pt-loaded alumina (Pt/alumina) catalyst [1] could detect hydrogen ( $\text{H}_2$ ) gas for wide concentration range from extremely low as 0.5 ppm, up to high as 5 vol.%  $\text{H}_2$  in air, and showed a good linearity between the  $\text{H}_2$  concentration in air and the sensing signal at the catalyst temperature of 100 °C [2].

Not only for  $\text{H}_2$  but also for other inflammable gas, the micro-TGS can be a useful platform device, because it is possible to modify the catalyst of the micro-TGS for the target gas. We have demonstrated the micro-TGS for carbon monoxide (CO) detection by integrating CO combustion catalyst of Au/ $\text{TiO}_2$  on the micro-TGS [3].

Gold (Au) nanoparticles have been known as a highly efficient catalyst combustor [4–8]. Haruta et al. [4] have reported that Au nanoparticles (AuNPs) are remarkably active for the low-temperature oxidation of CO when they are highly dispersed and deposited on reducible metal–oxide–semiconductor. Since this frontier work, many applications of the Au catalyst for CO sensors have been reported [7, 9–11].

We have integrated on the microdevice the 3 wt%Au/ $\text{TiO}_2$  catalyst which was prepared by coprecipitation method as a promising CO combustion catalyst [8], and investigated the combustion performance of this catalyst on the microdevice [3]. This catalyst was active and combusted the CO and  $\text{H}_2$  effectively. The 3 wt%Au/ $\text{TiO}_2$  catalyst on the microdevice oxidized not only CO but also  $\text{H}_2$ , showing poor CO selectivity.

We have changed the oxide from  $\text{TiO}_2$  to  $\text{Co}_3\text{O}_4$  in the catalyst and the process of the catalyst from coprecipitation method to impregnation method of the catalyst to enhance the CO selectivity. We have prepared a 20 wt%Au/ $\text{Co}_3\text{O}_4$  catalyst and evaluated the combustion performance of this catalyst on the micro-TGS [12]. Although the combustion performance of the 20 wt%Au/ $\text{Co}_3\text{O}_4$  catalyst was still

M. Nishibori (✉) · W. Shin · N. Izu · T. Itoh · I. Matsubara  
National Institute of Advanced Industrial Science and  
Technology (AIST), Shimo-Shidami, Moriyama-ku,  
Nagoya 463-8560, Japan  
e-mail: m-nishibori@aist.go.jp

low, the stability and CO selectivity of this catalyst on the microdevice was improved as compared to that of the 3 wt% Au/TiO<sub>2</sub> catalyst.

In our previous studies, we used the wet chemical process by impregnation of metal oxide powder and aqueous solution of Au chloride for preparation of the CO combustion catalyst. In these processes, the dispersion of the Au particles was low, and the coagulation of the size of 100 nm was found [12]. There was little active surface area of the Au particles, and the combustion performance was not enough. On the other hand, high content of the Au particle could enhance the stability of the combustion catalyst on the microdevice [12]. To fabricate the micro gas sensor of high activity, selectivity, and stability, a new process of the catalyst preparation with large content of the well-dispersed nanosize particles is necessary.

Recently, many researchers have reported that the nanostructured metal–oxide–semiconductor is a promising candidate for gas sensor material which enhances the sensing performance. Patil et al. [13] have synthesized the Co<sub>3</sub>O<sub>4</sub> nanorods by using a chemical co-precipitation/digestion method, and have demonstrated the CO sensing performance of the Co<sub>3</sub>O<sub>4</sub> nanorods as the sensing material. Calestani et al. [14] have optimized the standard vapor phase growth process for ZnO tetrapods, and have tested the sensing performance of the obtained ZnO tetrapods-based gas sensors with several gases. Furthermore, Liu et al. [15] have synthesized the porous  $\alpha$ -Fe<sub>2</sub>O<sub>3</sub> which was employed as a support for loading AuNPs, and have showed that the AuNp-supported porous  $\alpha$ -Fe<sub>2</sub>O<sub>3</sub> exhibited a much higher response in comparison to pure  $\alpha$ -Fe<sub>2</sub>O<sub>3</sub>.

The purpose of this work is to develop the CO combustion catalyst of Au/Co<sub>3</sub>O<sub>4</sub> which contains high content of Au over several tens % and the better dispersion of the AuNps for micro gas sensor application. In this study, we have prepared a highly dispersed Au/Co<sub>3</sub>O<sub>4</sub> catalyst by the mixing of Au colloid and cobalt oxide powder directly [8, 16], and evaluated the combustion performance on the microdevice. We have discussed the relationship between the microstructure and the combustion performance of the catalyst with the results of X-ray diffraction and the transmitted electron microscopy analysis on the catalysts with different Au contents.

## Experimental

Figure 1a shows the preparation process of the Au/Co<sub>3</sub>O<sub>4</sub> catalyst. The Au/Co<sub>3</sub>O<sub>4</sub> catalyst was prepared by mixing an aqueous solution dispersed with the colloid of Au metal particles (Tanaka Kikinzoku Kogyo K.K., mercaptosuccinic acid, Au content 2 wt%, average particle size of 3 nm)

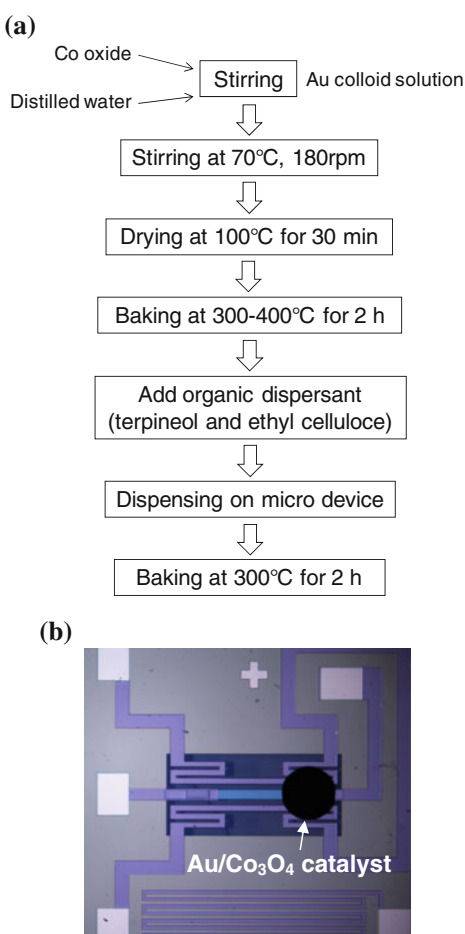


**Fig. 1** **a** Flow chart of catalyst powder preparation and the integration on the microdevice of Au/Co<sub>3</sub>O<sub>4</sub> catalyst. **b** A photo of the Au/Co<sub>3</sub>O<sub>4</sub> catalyst integrated on the microdevice

and a commercial cobalt oxide (Co<sub>3</sub>O<sub>4</sub>) powder (Aldrich, cobalt (II, III) oxide, nanopowder, 99.8%, particle size of 20–30 nm). The Au contents in the powder of Au/Co<sub>3</sub>O<sub>4</sub> catalyst were varied to be 3, 10, 20, and 40 wt%.

The Au colloid solution was stirred constantly, and then the Co<sub>3</sub>O<sub>4</sub> nanopowder was added to the solution, and then distilled water was added. The mixture solution was stirred at the temperature of 70 °C until the water evaporated. The obtained solid residue was dried at 100 °C for 30 min. The solid residue was baked again in air at 300–400 °C for 2 h to obtain catalyst powder.

Furthermore, the Au/Co<sub>3</sub>O<sub>4</sub> catalyst was also prepared by impregnation of a commercial cobalt oxide powder (Aldrich, cobalt (II, III) oxide, nanopowder, 99.8%, 20–30 nm) with an aqueous solution of HAuCl<sub>4</sub>·4H<sub>2</sub>O. The slurries were stirred at 100 °C for 30 min, and then dried at 120 °C for 2 h in air. The solid residue was baked again in air at 300 °C for 2 h to obtain catalyst powder.

For the evaluation of the combustion performance of the catalyst, the micro-TGS was used. A catalyst paste was

prepared by mixing the Au/Co<sub>3</sub>O<sub>4</sub> powder and an organic dispersant. The organic dispersant was a mixture of terpineol and ethyl cellulose with the weight ratio of 9:1. We integrated the Au/Co<sub>3</sub>O<sub>4</sub> catalyst on the thin membrane of the micro-TGS device by dispensing the catalyst paste and a drop of the catalyst paste was deposited using an air dispenser (MUSASHI Engineering Inc.). The size of the drop of the catalyst paste on the microdevice was controlled to be 0.6 mm in diameter by changing the dispensing time and air pressure. The deposited catalyst paste on the microdevice was baked in air at 300 °C for 2 h. Figure 1b shows a photo of the catalyst integrated on the device.

The combustion performance of the catalyst was investigated using a gas-flow-type test chamber with the chamber volume of 60 mL. During the test of gas combustion, the catalyst was heated up from 120 to 240 °C by the micro-heater of the micro-TGS flowing DC current. The response of the microdevice was measured by flowing alternately air and gas-air mixture; (i) 1 vol.% CO in air, (ii) 1 vol.% H<sub>2</sub> in air, and (iii) the gas mixture of 1 vol.% CO and 1 vol.% H<sub>2</sub> in air, into the sample test chamber at the gas flow rate of 200 mL/min.

The relative amount of the combustion heat from the catalyst on the microdevice was estimated by the voltage signal of the device generated from the thermoelectric energy conversion of the SiGe thin film pattern of the device. The voltage signal of the micro-TGS ( $\Delta V$ ) is directly related to the combustion performance of the catalyst ( $\Delta T$ ) as follows,

$$\Delta V = \alpha \Delta T,$$

where  $\alpha$  is Seebeck coefficient of the thermoelectric pattern of SiGe in the micro-TGS, which does not depend on the device shape. In this report, we used the voltage signal ( $\Delta V$ ) of the micro-TGS as an index of combustion performance of the catalyst on the device. We have monitored the raw date of the voltage signal without the amplifier circuit using the digital multimeter (Keithley 2700, 6.5 digit, resolution of 22 bit).

The CO selectivity,  $S_{CO}$ , of the Au/Co<sub>3</sub>O<sub>4</sub> catalyst can be represented by the ratio of the combustion performance of the CO gas to that of the H<sub>2</sub> gas as follows,

$$S_{CO} = \Delta V_{CO} / \Delta V_{H_2},$$

where  $\Delta V_{CO}$  and  $\Delta V_{H_2}$  is the voltage signal of the micro-TGS to the CO and H<sub>2</sub> gas, which is defined as the index of the combustion performance of the catalyst.

The characterization and the microstructural observation of the Au/Co<sub>3</sub>O<sub>4</sub> catalyst was carried out using an X-ray diffractometer with Cu K $\alpha$  irradiation (XRD; Rigaku, RINT2100) and a transmitted electron microscope (TEM; JEOL, JEM2010), respectively.

## Results and discussion

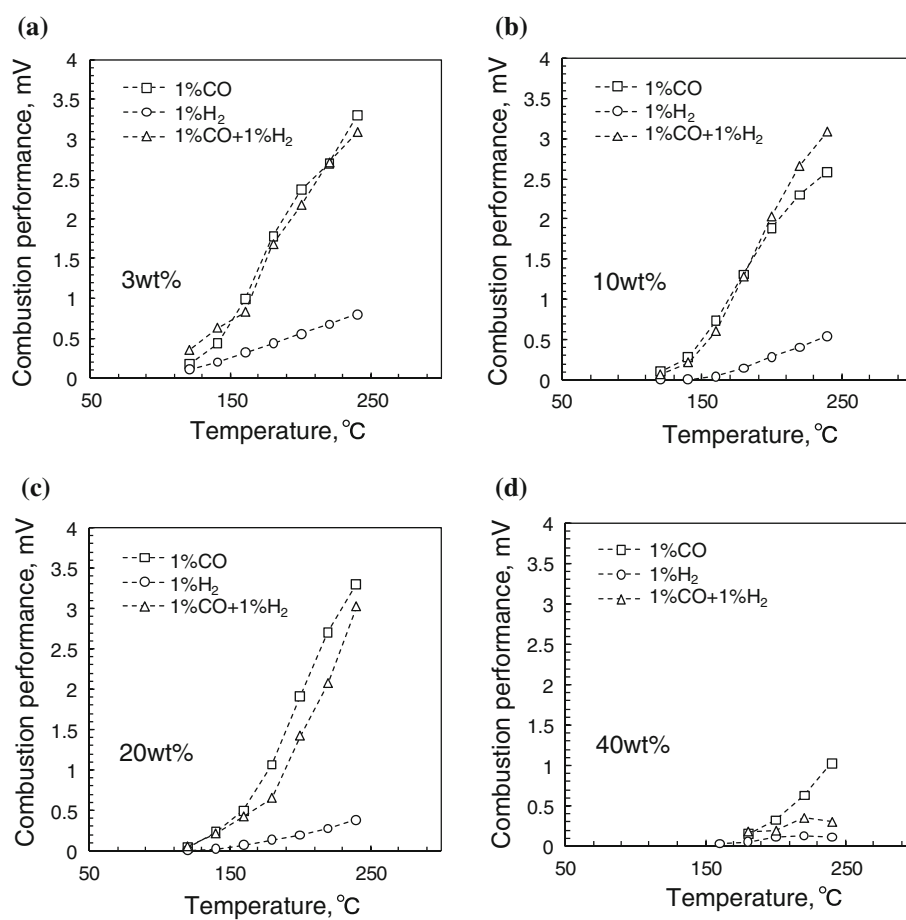
### Combustion performance

Figure 2 shows the temperature dependence of the combustion performance of the Au/Co<sub>3</sub>O<sub>4</sub> catalyst with different Au contents, (a) 3 wt%, (b) 10 wt%, (c) 20 wt%, and (d) 40 wt%, for 1 vol.% CO, 1 vol.% H<sub>2</sub>, the gas mixture of 1 vol.% CO and 1 vol.% H<sub>2</sub> in air. The combustion performance of the catalysts of Au content with 3, 10, and 20 wt% were larger than that with 40 wt% to all gases. For 1 vol.% CO in air, the 3, 10, and 20 wt%Au/Co<sub>3</sub>O<sub>4</sub> catalysts burned CO at the catalyst temperature over 120 °C and the combustion performance increased with the catalyst temperature. The 40 wt%Au/Co<sub>3</sub>O<sub>4</sub> catalyst burned CO at the catalyst temperature over 180 °C and the combustion performance was smaller than that of 3, 10, and 20 wt%Au/Co<sub>3</sub>O<sub>4</sub> catalyst. The combustion performance of these catalysts for 1 vol.% H<sub>2</sub> in air also changed with the Au content of the catalyst, and was considerably less than that of 1 vol.% CO in air. For the mixture gas of 1 vol.% CO and 1 vol.% H<sub>2</sub> in air, the combustion performance of the 3 and 10 wt%Au/Co<sub>3</sub>O<sub>4</sub> catalysts was the same to that of 1 vol.% CO in air. On the other hand, the combustion performance of the 20 and 40 wt%Au/Co<sub>3</sub>O<sub>4</sub> catalysts decreased slightly in comparison with that of 1 vol.% CO in air. The mixture gas of CO and H<sub>2</sub> in air effects depend on the combustion performance of the Au/Co<sub>3</sub>O<sub>4</sub> catalyst. This behavior could be explained by the deactivation of the active sites of the catalyst by oxidized substances (H<sub>2</sub>O and/or CO<sub>2</sub>), and the change of the degree of competing absorption by H<sub>2</sub> and CO. In the case of the 40 wt%Au/Co<sub>3</sub>O<sub>4</sub> catalyst with low combustion performance, the dissipation of the combustion heat by the test gas including H<sub>2</sub> could not be negligible.

Table 1 shows the summary of the combustion performance of the Au/Co<sub>3</sub>O<sub>4</sub> catalysts with different Au content, which are prepared by impregnation process and colloid process. For 1 vol.% CO in air, the combustion performance of the 3 wt%Au/Co<sub>3</sub>O<sub>4</sub> catalyst prepared by colloid process has increased to 2.37 mV while that of the catalyst prepared by impregnation process was 0.114 mV at 200 °C. The combustion performance of the 20 wt%Au/Co<sub>3</sub>O<sub>4</sub> catalyst prepared by colloid process has increased to 1.92 mV while that of the catalyst prepared by impregnation process was 0.217 mV at 200 °C. These results tell that the CO combustion performance of the Au/Co<sub>3</sub>O<sub>4</sub> catalyst has been improved by the colloid process of the catalyst preparation, which conducted effective mixing of Au colloid and cobalt oxide powder.

The CO selectivity,  $S_{CO}$ , of the Au/Co<sub>3</sub>O<sub>4</sub> catalyst can be represented by ratio of the combustion performance of CO and H<sub>2</sub>. Table 2 shows the CO selectivity of the 3,

**Fig. 2** Temperature dependence of the combustion performance of the Au/Co<sub>3</sub>O<sub>4</sub> catalysts with the different Au content of **a** 3 wt%, **b** 10 wt%, **c** 20 wt%, and **d** 40 wt% for 1 vol.% CO, 1 vol.% H<sub>2</sub> and the gas mixture of 1 vol.% H<sub>2</sub> and 1 vol.% CO in air at the gas flow rate of 200 ccm



**Table 1** Combustion performance (relative amount of the combustion heat from the catalyst on the microdevice represented by the voltage signal from the thermoelectric conversion) of the Au/Co<sub>3</sub>O<sub>4</sub> catalyst with different Au content

T <sub>catalyst</sub> (°C)	Gas	Combustion performance, ΔV (mV)							
		Au content 3 wt%		Au content 10 wt%		Au content 20 wt%		Au content 40 wt%	
		IMP	Colloid	IMP	Colloid	IMP	Colloid	IMP	Colloid
240	1% CO	3.30		2.59		3.03		1.03	
	1% H <sub>2</sub>	0.81		0.54		0.39		0.12	
220	1% CO	2.69		2.30		2.71		0.63	
	1% H <sub>2</sub>	0.68		0.40		0.28		0.13	
200	1% CO	0.114	2.37	1.89	0.217	1.92		0.32	
	1% H <sub>2</sub>	0.041	0.56	0.28	0.104	0.2		0.11	
180	1% CO		1.78	1.31		1.07		0.15	
	1% H <sub>2</sub>		0.44	0.14		0.14		0.05	
160	1% CO	0.037	1.00	0.72	0.043	0.50			
	1% H <sub>2</sub>	NA	0.32	0.04	0.006	0.08			
140	1% CO		0.44	0.27		0.24			
	1% H <sub>2</sub>		0.19	0.01		0.03			
120	1% CO	0.013	0.17	0.09	0.009	0.04			
	1% H <sub>2</sub>	NA	0.10	0.01	NA	0.01			

Impregnation (IMP) and colloid represent the preparation method of the catalyst by impregnation process in our previous study and colloid process in this study

**Table 2** CO selectivity ( $S_{CO}$ ) ratio of the combustion performance of CO and H<sub>2</sub>, of the Au/Co<sub>3</sub>O<sub>4</sub> catalyst with the Au content of 3, 10, 20, and 40 wt%

$T_{catalyst}$ (°C)	CO selectivity, $S_{CO}$			
	Au content 3 wt%	Au content 10 wt%	Au content 20 wt%	Au content 40 wt%
240	4.07	4.80	7.77	8.58
220	3.96	5.75	9.68	4.85
200	4.23	6.75	9.60	3.00

10, 20, and 40 wt% Au/Co<sub>3</sub>O<sub>4</sub> catalysts, which was estimated from the combustion performance listed in Table 1. The CO selectivity of the Au/Co<sub>3</sub>O<sub>4</sub> catalyst at the catalyst temperature of 200 °C was higher than that of the catalyst temperature of 240 °C, except for the Au content of 40 wt%. The CO selectivity of the Au content of 20 wt% was higher than that of the Au content of 3, 10, and 40 wt%. At the catalyst temperature of 200 °C, the CO selectivity of the catalyst with the Au content of 3, 10, 20, and 40 wt% were 4.23, 6.75, 9.60, and 3.00, respectively.

The Au/Co<sub>3</sub>O<sub>4</sub> catalyst of the Au content of 3 wt% showed the high combustion performance to not only CO gas but also H<sub>2</sub> gas. On the other hand, the CO combustion performance of the Au content of 20 wt% was closed to the same performance of the Au content of 3 wt%, and is of high selectivity. These results suggest that the combustion performance and selectivity of the Au/Co<sub>3</sub>O<sub>4</sub> catalyst on the microdevice to the CO gas can be improved by the Au content. In particular, the Au content of 20 wt% shows high combustion performance and selectivity on the microdevice.

#### Microstructure

Figure 3 shows the XRD patterns of the Au/Co<sub>3</sub>O<sub>4</sub> catalysts with the different Au content with (a) 3 wt%, (b) 10 wt%, (c) 20 wt%, and (d) 40 wt%, which were prepared by the colloid process. The average grain size of the Au particles in the catalyst could be calculated from the peak broadening, and increased with the Au content of the catalyst. The calculated grain size of Au particle in the Au/Co<sub>3</sub>O<sub>4</sub> catalyst was 9, 14, 17, and 34 nm for 3, 10, 20, and 40 wt%, respectively.

Figure 4 shows the TEM images of the Au/Co<sub>3</sub>O<sub>4</sub> catalysts with the Au content of (a) 3 wt%, (b) 10 wt%, (c) 20 wt%, and (d) 40 wt%, which were prepared by the colloid process. The large bright features of 20–30 nm are Co<sub>3</sub>O<sub>4</sub> particles. The dark features of the size of 5–15 nm in TEM images attached on the Co<sub>3</sub>O<sub>4</sub> are Au particles. The grain size of the Au particle in the Au/Co<sub>3</sub>O<sub>4</sub> catalyst

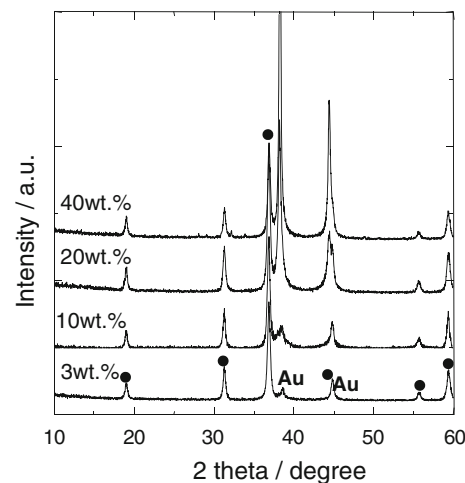


**Fig. 3** XRD patterns of the Au/Co<sub>3</sub>O<sub>4</sub> catalysts of the different Au content with (a) 3 wt%, (b) 10 wt%, (c) 20 wt%, and (d) 40 wt%. The peak patterns of Co<sub>3</sub>O<sub>4</sub> (circle) and Au metal (Au) are indicated

was around 4, 10, 13, and 30 nm for 3, 10, 20, and 40 wt%, respectively. The grain size of the Au particles in these images was smaller than that calculated from the XRD peak broadening. This difference is result from the fact that the calculated size of Au particles from the XRD peak broadening is the average grain size of the Au particles including the particle coagulation. As shown in Fig. 4, there was no obvious difference of the grain sizes of the Au particles between the Au content of 10 and 20 wt%, though the particle coagulation of the size of 20–30 nm was found a little for the Au content of 20 wt%. The dispersion of the Au particles in the Au content of 40 wt% was bad, and the particle coagulation of the size of 50 nm was found as shown in Fig. 4d. The summary of the particle size of the Au/Co<sub>3</sub>O<sub>4</sub> catalyst and the BET surface area are listed in Table 3.

The initial size of Au particles of Au colloid was an average of 3 nm. In this study, the average grain size of the Au particles of the 10 wt% Au/Co<sub>3</sub>O<sub>4</sub> was around 4 nm, and has slightly grown. The Au particles of the Au content of 10 and 20 wt% aggregated and caused the grain growth to the size of 5–15 nm. This grain size of the Au particle of the Au content of 20 wt% was 1/10 of that by the catalyst with the same composition prepared by impregnation process in our previous studies. The process of the catalyst preparation by the mixing of Au colloid and cobalt oxide powder could realize a better dispersion of Au particles in the dispersed Au/Co<sub>3</sub>O<sub>4</sub> catalyst. The combustion performance of the Au content of 20 wt% was enhanced by the improvement of microstructure using the catalyst preparation of colloid process, and was 10 times higher than that of the catalyst prepared by the impregnation process in our previous study.

**Fig. 4** TEM images of Au/ $\text{Co}_3\text{O}_4$  catalysts with the different Au content of **a** 3 wt%, **b** 10 wt%, **c** 20 wt%, and **d** 40 wt%. The bright features are  $\text{Co}_3\text{O}_4$  particles and the dark features are Au particles

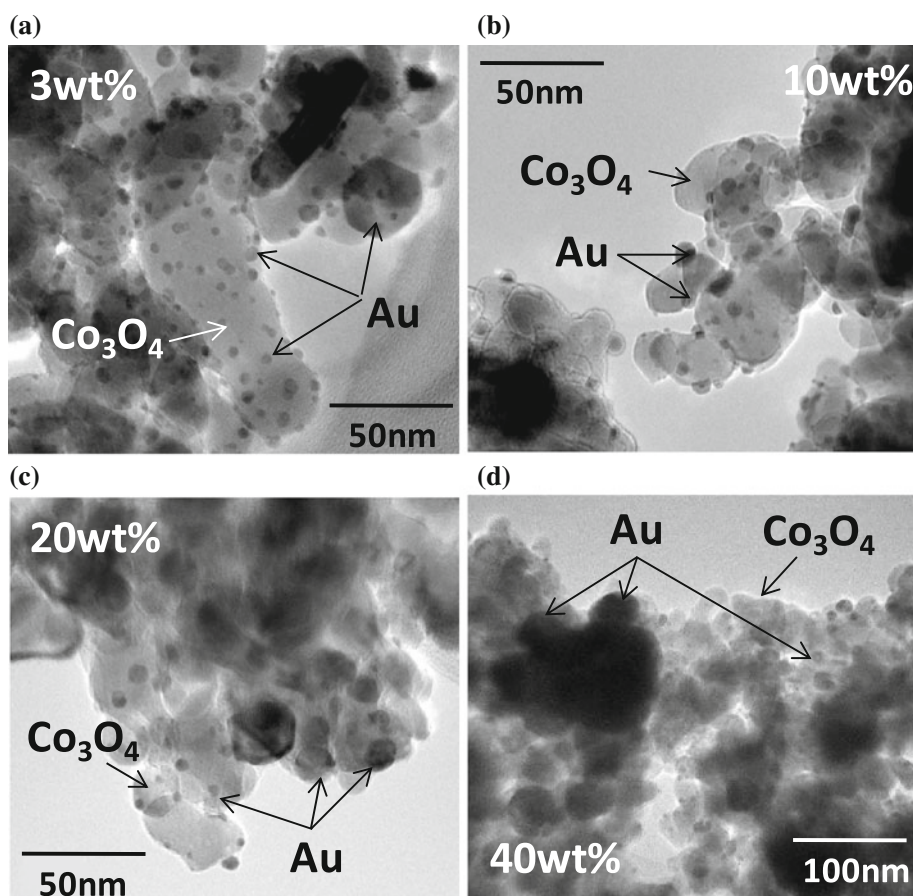


**Table 3** Summary of the particle size and the BET surface area of the Au/ $\text{Co}_3\text{O}_4$  catalyst prepared by colloid process

	Particle size by TEM		Surface area by BET ( $\text{m}^2/\text{g}$ )
	Au (nm)	$\text{Co}_3\text{O}_4$ (nm)	
3 wt%Au/ $\text{Co}_3\text{O}_4$	4	35	28.8
10 wt%Au/ $\text{Co}_3\text{O}_4$	10	30	31.6
20 wt%Au/ $\text{Co}_3\text{O}_4$	13	30	30.5
40 wt%Au/ $\text{Co}_3\text{O}_4$	30	24	19.9

The activity of Au catalyst is dependent on the grain size of Au particles, and the nanoparticle with the grain size of less than 10 nm provides better performance [17]. Therefore, the 40 wt%Au/ $\text{Co}_3\text{O}_4$  catalyst seemed to be rather inactive and the combustion performance of this catalyst was low. In this study, the Au particle size of less than 10 nm was only observed in the 3 wt%Au/ $\text{Co}_3\text{O}_4$  catalyst. Although the Au particle size of the 10 and 20 wt%Au/ $\text{Co}_3\text{O}_4$  catalyst was  $\sim$ 13 nm, the CO combustion performance of these catalysts on the microdevice was as high as that of the 3 wt%Au/ $\text{Co}_3\text{O}_4$  catalyst.

We suggest that the good combustion performance obtained for the 10 and 20 wt%Au/ $\text{Co}_3\text{O}_4$  catalyst on the

microdevice is attributed to the increase of the number of the active site depending on the amount of Au content even though the catalytic activity of each Au particle is not as high as that of the 3 wt%Au/ $\text{Co}_3\text{O}_4$  catalyst. We kept constant the volume of the catalyst integrated on the microdevice using the air dispenser because of the evaluation of the combustion performance across the catalyst on the microdevice. The density of the Au/ $\text{Co}_3\text{O}_4$  catalyst changes depending on the content of Au loaded  $\text{Co}_3\text{O}_4$ . Therefore, the number of the Au particles on the device has increased with the content of Au loaded  $\text{Co}_3\text{O}_4$ . On the other hand, for the 40 wt%Au/ $\text{Co}_3\text{O}_4$  catalyst, the large Au particle seemed to be rather inactive and the combustion performance of this catalyst was low.

Figure 5 shows the difference of the catalytic performance of the 3, 10, 20, and 40 wt%Au/ $\text{Co}_3\text{O}_4$  catalyst on the microdevice at the catalyst temperature of 200 °C. For 1 vol.% CO in air, the catalytic performance of the Au/ $\text{Co}_3\text{O}_4$  catalyst on the microdevice did not change within the range of Au content from 3 to 20 wt%. On the other hand, for 1 vol.% H<sub>2</sub> in air, the catalytic performance on the microdevice decreased significantly with the Au content of the catalyst, and was decreased 50% in the range of the Au content of 10–20 wt%. The catalytic performance of the

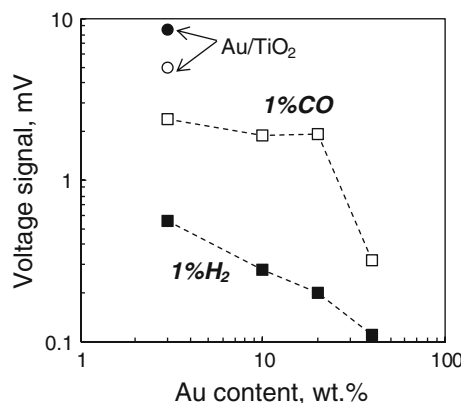


**Fig. 5** Difference of the catalytic performance of the 3, 10, 20 and 40 wt% Au/Co<sub>3</sub>O<sub>4</sub> catalyst on the microdevice at the catalyst temperature of 200 °C (filled square, open square). The results of our previous study using 3 wt% Au/TiO<sub>2</sub> catalyst (filled circle, open circle) also are indicated

40 wt% Au/Co<sub>3</sub>O<sub>4</sub> catalyst was low to the CO gas and inactive to the H<sub>2</sub> gas. As a result, the CO selectivity,  $S_{CO}$ , changed depending on the Au content of the catalyst which corresponds to the grain size of Au particle. We can consider that the CO selectivity of the Au/Co<sub>3</sub>O<sub>4</sub> catalyst on the microdevice was highest at the Au content of 20 wt% (Au particle size of ~15 nm) because the H<sub>2</sub> combustion performance of the Au/Co<sub>3</sub>O<sub>4</sub> catalyst depends greatly on the Au particle size compared with the CO combustion performance. The CO selectivity is also dependent on the kind of metal oxide. Although the combustion performance of the Au/TiO<sub>2</sub> catalyst is larger than that of the Au/Co<sub>3</sub>O<sub>4</sub> catalyst, the Au/TiO<sub>2</sub> catalyst has no CO selectivity to H<sub>2</sub>.

Schubert et al. [18] has shown that the Au particle size of the Au/Co<sub>3</sub>O<sub>4</sub> catalyst was around 3.4 nm and their catalyst showed high selectivity but strong deactivation. Our results of the 20 wt% Au/Co<sub>3</sub>O<sub>4</sub> catalyst showed the high selectivity though the Au particle size of the catalyst, ~13 nm, is larger than that reported by Schubert et al. [18]. The deactivation of the Au/Co<sub>3</sub>O<sub>4</sub> catalyst is an important problem and seems to occur by forming of the thin layer of the carbonate on the catalyst surface. In the future, we will investigate an influence of the Au content and particle size on the probability of the performance degradation which is caused by the physical covering of the Au particles with the carbonate.

## Conclusion

The CO combustion catalysts of Au loaded on Co<sub>3</sub>O<sub>4</sub> which contains large amounts of Au (3, 10, 20, and 40 wt%) for the integration on the microdevice were developed and the combustion performance of these

catalyst was evaluated on the microdevice. The grain size of Au particle in the Au/Co<sub>3</sub>O<sub>4</sub> catalyst was 4, 10, 13, and 30 nm for 3, 10, 20, and 40 wt%, respectively. The Au particle size of the Au content of 20 wt% was 1/10 of that by the catalyst with the same composition prepared by impregnation process in our previous studies, and the combustion performance of this catalyst was improved by 10 times higher than that reported in our previous study.

There were no difference in the combustion performance of CO in air between the Au content of 3, 10, and 20 wt%, though the combustion performance of H<sub>2</sub> in air decreased significantly with the Au content of the catalyst. As a result, the CO selectivity was also dependent on the Au content of the catalyst, and was the highest in the Au content of 20 wt%.

In the application of the gas sensor, not only the combustion performance of the catalyst but also selectivity is an important factor. The Au/Co<sub>3</sub>O<sub>4</sub> catalyst prepared by colloid method in this study showed high catalytic performance and CO selectivity on the microdevice. The thermoelectric gas sensor with the Au/Co<sub>3</sub>O<sub>4</sub> catalyst in this study could be an excellent CO gas sensor.

**Acknowledgements** The authors are grateful to Dr. Y. Tai of the AIST for useful discussion about the catalytic activity. We thank Dr. T. Miki of the AIST for evaluating the BET surface area.

## References

- Shin W, Choi Y, Tajima K, Izu N, Matsubara I, Murayama N (2005) Sens Actuators B 108:455
- Nishibori M, Shin W, Houlet LF, Tajima K, Izu N, Itoh T, Murayama N, Matsubara I (2006) J Ceram Soc Japan 114:853
- Nishibori M, Tajima K, Shin W, Izu N, Itoh T, Matsubara I (2006) J Ceram Soc Japan 115:34
- Haruta M, Kobayashi T, Sano H, Yamada N (1987) Chem Lett 2:405
- Haruta M, Yamada N, Kobayashi T, Iijima S (1989) J Catal 115:301
- Haruta M, Tsubota S, Kobayashi T, Kagayama H, Genet MJ, Delmon B (1993) J Catal 144:175
- Kobayashi T, Haruta M, Tsubota S, Sano H (1990) Sens Actuators B 1:222
- Tsubota S, Nakamura T, Tanaka K, Haruta M (1998) Catal Lett 56:131
- Hashimoto A, Hibino T, Kobayashi K, Sano M (2003) Electrochemistry 71:398
- Choi US, Sakai G, Shimomae K, Yamazoe N (2005) Sens Actuators B 107:397
- Matsunaga M, Qiu F, Shin W, Izu N, Matsubara I, Murayama N, Kanzaki S (2004) J Electrochem 151(1):H7
- Nishibori M, Shin W, Houlet LF, Tajima K, Itoh T, Izu N, Matsubara I (2007) J Ceram Soc Japan 115:748
- Patil D, Patil P, Subramanian V, Joy P, Potdar H (2010) Talanta 81:37
- Calestani D, Zha M, Mosca R, Zappettini A, Carotta MC, Natale VDi, Zanotti L (2010) Sens. Actuators B 144:472

15. Liu X, Zhang J, Guo X, Wu S, Wang S (2010) Nanotechnology 21:1
16. Choi Y, Tajima K, Shin W, Izu N, Matsubara I, Murayama N (2006) J Mater Sci 41:2333. doi:[10.1007/s10853-006-7154-y](https://doi.org/10.1007/s10853-006-7154-y)
17. Lim DC, Lopez-Salido I, Dietshe R, Bubek M, Kim YD (2006) Angew Chem Int Ed 45:2413
18. Schubert MM, Plzak V, Garche J, Behm RJ (2001) Catal Lett 76:143